

CONSERVATION OF THE MURAL PAINTINGS AT THE THEBAN TOMB TT 340
AT DEIR EL- MEDINA NECROPOLIS, WESTERN THEBES, LUXOR, EGYPT

Manci, A.^(*) & Sedikk, M.

Conservation dept., Faculty of Archaeology and Tourism Guidance, Misr University for Science & Technology, 6th October, Egypt

E-mail address: ahmed.ibrahim@must.edu.eg

Article info.

EJARS – Vol. 13 (1) – June 2023: 27-46

Article history:

Received: 9-9-2022

Accepted: 14-6-2023

Doi: 10.21608/ejars.2023.305185

Abstract:

This research aims to study the characteristics and technique of mural painting at the tomb of Amenemhat (No. 340), assessment of its current conservation state, moreover select and apply the most suitable materials and methods to conservation. The characterization of the mural paintings in the studied tomb was carried out using different techniques including visual examination, portable USB-Digital microscope; polarizing light microscope; scanning electron microscopy (SEM) equipped with energy dispersive x-ray analysis system (SEM-EDS); x-ray powder diffraction (XRD), and Fourier transform infrared spectroscopy (FTIR). In order to select the optimal materials for consolidation and completion processes, an experimental study was carried out using various methods including visual examination, scanning electron microscopy (SEM) and colorimetric measurements. The results indicated that the ancient Egyptian artist used the traditional technique (tempera) which is used inside the rock tombs for preparing the wall paintings at the tomb of Amenemhat (No. 340). The mural paintings in the tomb are suffering from the influence of many indigenous and exogenous deterioration factors. The results of experimental tests demonstrated that the product of Klucel G 1% has high efficiency in the consolidation of the weak painting layer. Also; the product of Bio Estel has high efficiency in the consolidation of fragile mud plaster layers. Moreover, the data clarified that the mortar (1) which consists of 0.5 rough yellow sand, 0.5 fine yellow sand, 3 light mud, 1 heba powder, 0.5 burned clay, 1 straw, 3 gm Tobsin N and distilled water it's a suitable for filling gaps and cracks in the mural paintings. Finally, treatment procedures were successfully performed using pre-consolidation, mechanical cleaning, re-adhesion of partly det-ached and flaking layers, consolidation, filling gaps and missing parts and cracks injections.

Keywords:

Mural paintings

Theban tomb

Mud brick

Mud plaster

Pigments

Deterioration

Conservation

1. Introduction

1.1. Archaeological background

The city of workers at Deir el-Medina lies on the west bank of Luxor in a small desert valley behind the Qurnet Murai hill slope, between the valley of the kings to the north and valley of the queens to the west, close to the Ramesseum and Medinet Habu, and well away from the cultivation. It's a walled village in the form of a trapezoid roughly 5,600 m², containing of 68 houses separated by a road running the

length of the village, with a gate at the north end [1]. It was built to house the workmen that were employed by the state to build and decorate the royal tombs in western Thebes during the new kingdom (ca. 1550-1069 BCE), and their families and servants. The city is surrounded by eastern and a western cemetery. To the east lies the 18th dynasty cemetery. The western cemetery contains a small number

of 18th dynasty tombs but is predominantly 19th and 20th dynasty in date, fig (1) [2-4]. One of the unique tombs in the eastern cemetery of Deir el-Medina is Amenemhat tomb (No. 340). Amenemhat is a workman from Deir el-Medina who lived in the 18th dynasty during the new kingdom. The tomb was discovered by a French archaeologist Bernard Bruyère (1879-1971), on 13 March 1925. It's probably the oldest craftsmen tomb in the area. The tomb layout is quite simple. It's a tiny rectangular and vaulted ceiling chapel, with long axis perpendicular to the entrance passage with a small courtyard, fig. (1). The courtyard is now largely destroyed; only the south wall is still original. There is a small niche dug into the west wall with a rounded top. The tomb contains of unfinished funerary and religious decorations (offerings, funeral procession). Where only the decoration of the western, southern walls and ceiling has been completed, while the decorations of the northern and eastern walls are incomplete [5].

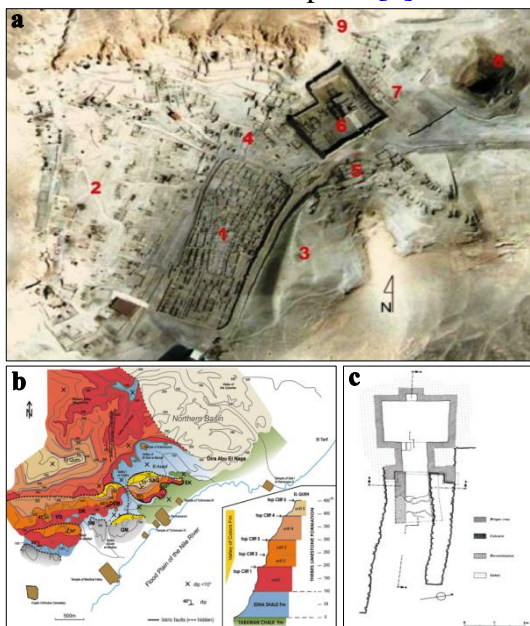


Figure (1) Shows **a.** site of Deir el-Medina; 1. the village; 2. western cemetery; 3. eastern cemetery; 4. votive chapels; 5. Ramesside cemetery; 6. Ptolemaic Hathor temple; 7. Hathor chapel of Sety I; 8. great pit; 9. tombs of Saite (After: Jaana, 2011), **b.** geological map of the west bank and its stratigraphical succession (After: Dupuis, 2011) **c.** plan of the tomb 340 at Deir el Medina (After: Cherpion, 1999),

1.2. Geological background

Geologically, the bedrock of the west bank of Luxor is formed by three main formations, >350 m thick: **1) Tarawan chalk formation at the base;** **2) Esna shale formation at the middle;** and **3) Thebes limestone formation at the top.** The Tarawan chalk formation consists of a soft, white, fine-grained limestone with isolated flint layers. Tarawan chalk formation is not currently known in outcrop on the west bank except at a few locations. The Esna shale formation, with a total thickness of >60 m at Thebes west, it is a heterogeneous succession, composed mainly of greenish shale with abundant anhydrite nodules, some millimeter-thin, and fine-grained sand layers. This formation has been subdivided into four formal members (Abu Had Mbr, El- Mahmiya Mbr, Dababiya Quarry Mbr, and El Hanadi Mbr). The overlying geological units are Thebes Limestone Formation, with a total thickness of >270 m in the form of five units richly fossiliferous, composed of an alternating series of limestone, marls, brecciated marls, shales and nodular chalks with interbedded chert nodules and chert bands. The hills of Deir el Medina were formed of ~18 m of shale of the Abu Had member of the Esna Shale formation overlain by the massive limestones of unit 1 of the Thebes limestone formation. A complete succession through the Thebes limestone formation up to the lower part of unit 4 constitutes the bulk of the hills [6-8]. There are no studies available about the materials and techniques of mural paintings at the tomb of Amenemhat (No. 340), current conservation state or previous conservation works. This research aims to study the characteristics and technique of mural painting in the studied tomb, assessment of current conservation state, select and apply the most suitable materials and methods to conservation. The properties of the mural paintings samples were determined by means of visual examination, polarizing microscope, scanning electron microscope, portable USB-digital microscope, X-ray diffraction, EDX, and FTIR

respectively. The conservation materials were evaluated by visual examination, colorimetric measurements, and morphological characterization using SEM. The results obtained from this work will provide much information concerning the materials and painting techniques used during that period of the ancient Egyptian history, and it will provide many important information about the appropriate conservation materials of the mural paintings at the tomb of Amenemhat (No. 340), that is probably useful in the conservation of the mural paintings which they have a similar characterizations and conditions.

2. Condition Assessment

The visual observations of studied wall paintings revealed that the yellow background of figures up on the vaulted ceiling is more vivid than the yellow background of the other walls. Existence of preparatory drawing by white color on the unfinished north side of the eastern wall was also observed. Unlike the drawings on the western and southern walls there are no outlines around the figures in the north and east walls. Many corrections of the decoration executed by yellow and red pigments were observed, fig. (2).

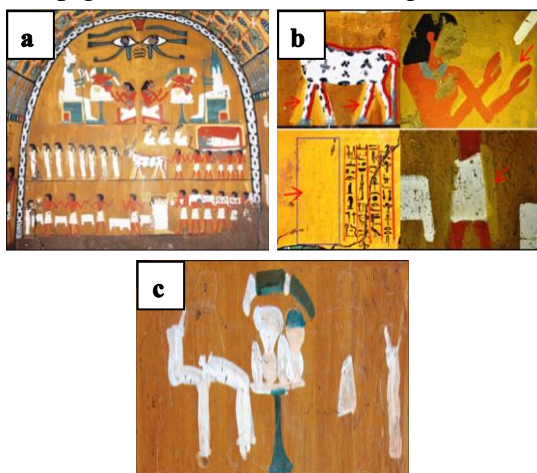


Figure (2) Shows **a.** decoration of the north wall, **b.** corrections of the decorations, **c.** the preparatory drawing was applied by white pigment on the yellow background.

The visual observations of Amenemhat's tomb (No 340), led to diagnose the degradation forms that occurred of the wall

paintings as a result to the influence of deterioration factors. Where tiny holes for insects have been observed in the mural painting layers (mud brick and mud plaster). In addition, superficial deposits of dome-shaped wild wasps' nests, formed of mud mixed with adhesive and fixed on the surfaces of murals, fig. (3-a). There is a thin layer of dust and fine particulates deposited on the surface of murals. Moreover, there are large structural gaps in the mural paintings, fig. (3-b). Some parts of the murals are suffered from paint loss, powdering, besides the voluntary losing of the paint layer in all the eyes and most faces of the characters. Many horizontal and vertical cracks have been observed in the wall paintings and some of which pierce all layers along the walls, fig. (3-c). Furthermore, networks of micro cracks are spread on the surface of murals. There are detachments of the mud plaster from mud brick support (peeling) in some parts, and bulges of the lower parts of the walls also observed.

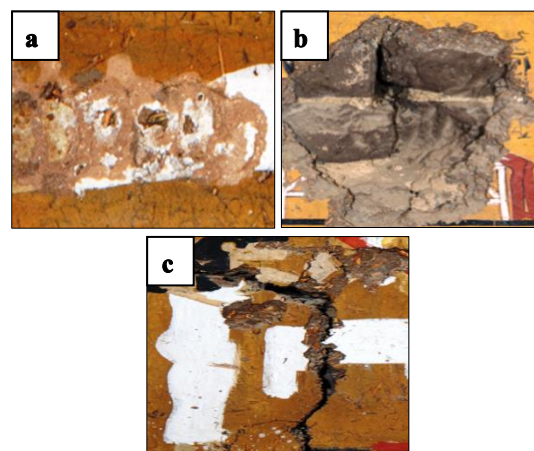


Figure (3) Shows **a.** deposits of wild wasps' nests, **b.** large structural gaps, **c.** vertical cracks are penetrate the wall painting layers

3. Materials and Methods

3.1. Materials

To characterize the mural paintings at the tomb of Amenemhat (No. 340), very small samples were collected from the fragments that have fallen as a result of deterioration mechanisms. The samples are representative to different visible colors, plaster layers, support, and mother rock, to provide the information about the stratigraphic of mural

paintings. Three consolidation products were evaluated to detect the most suitable product, which can be used to treat the painting layer: **1)** Klucel G 1% (Hydroxypropyl cellulose); **2)** Plexisol 550p 2% (A 40% solution of an acrylic resin based on Butyl methacrylate in benzene); **3)** Paroloid B72 3% (70% Ethyl methacrylate and 30% Methyl acrylate). Also three types of silicon based polymers were evaluated to detect the most suitable product, that can be used to consolidating the mud plaster layer: **1)** Estel 1100 is a product based on Ethyle silicate and Poly siloxane (CTS, Italy); **2)** Bio Estel is a product based on silicic acid esters modified with preservatives (CTS, Italy); **3)** Wacker OH 100, ethyl silicate & methyl ethyl ketone based product (Wacker Chemie, Germany).

3.2. Application

To simulate the consolidation treatment as it happens in the archaeological field, the consolidation materials were applied on experimental samples that were prepared with the same characteristics as the mural paintings in the tomb of Amenemhat (No. 340), using brushing until the surface was saturated and did not accept any more consolidant solution. Treated samples were left for 1 month at room temperature and controlled RH 50% to allow the polymerization process to take place [9-11]. To preparation mortars for filling gaps and joints of the mural paintings, local natural materials were used, including good quality yellow sand, which salt free, heba powder (a local clayey limestone found in the pockets of the geological setting of area), mud, shopped straw, burned clay, antifungal Tobsine M (Thiophanate- Methyl- 70% wettable powder), and distilled water. The experimental study was conducted on three types of mortar. The compositions and percentages of the prepared mortars are reported in tab. (1). Its different components were manually mixed in their dry states, finally; adding water as needed in order to obtain a suitable texture and volume for application. All mortar samples were tested

under the same environmental conditions, and had the same drying time (5 days).

Table (1) The compositions of the used mortars.

Mortar	Components %
(1)	1/2 rough yellow sand + 1/2 fine yellow sand + 3 light mud + 1 heba powder + 1/2 burned clay + 1 straw + 3 gm Tobsin N + distilled water.
(2)	1 rough yellow sand + 1 fine yellow sand + 3 light mud + 1 heba powder + 1 straw + 3 gm Tobsin N + distilled water.
(3)	1 rough yellow sand + 3 light mud + 1 heba powder + 1 straw + 3 gm Tobsin N + distilled water.

3.3. Analyses and investigations

Nikon eclipse LV100POL PM was used to describe the petrographic structure of the collected samples of the support and the plaster layers through the prepared thin sections. The portable USB-digital microscope model "VehoVMS-004 DELUXE" was used to determine the physical and stratigraphic structure of the studied mural paintings. It's a modern and advanced technology enables us to examine the mural layers without sampling. It has variable magnification the objects ranging from 20 to 500X. Quanta FEG 250 scanning electron microscope (SEM) was used to provide information about mineral morphology, crystals features, and to evaluating the consolidation treatments. The investigation was performed on non-coated samples. Moreover, the Micro chemical analysis of the collected samples was carried out using EDX unit attached with this microscope. The mineralogical composition for the collected samples was determined by means of x-ray diffraction analysis, which was performed using Philips analytical x-ray diffractometer. The operating conditions were gained through Cu α radiation. The spectra were collected from 2-60 2θ ; the scanning speed was $2\theta = 1$ degree/min, at constant voltage 40 kv, and 25 mA. The obtained XRD patterns and relative intensities were compared with the ICDD files. The organic binder (coloring media) that used in the coloring of the murals, was determined by means of fourier transform infrared spectroscopy (FTIR) analysis, by determine the organic functional groups present in the red painted sample. The analysis was performed using Bruker Vertex 80 (Germany) combined platinum diamond ATR, comprises

a diamond disk as that of an internal reflector in the range 4000- 400 cm^{-1} with resolution 4 cm^{-1} , refraction index 2.4. A colorimetric study was performed on the treated samples to identify the colour alterations due to the treatments, by means of UV-3101PC Scanning spectrophotometer, based on the L^* , a^* and b^* coordinates of the CIELAB color space. Where L^* is the lightness/darkness coordinate ($L^* = 0$ indicates black and $L^* = 100$ indicates diffuse white darkness), a^* the red/green coordinate ($+a^*$ indicating red and $-a^*$ green) and b^* the yellow/blue coordinate ($+b^*$ indicating yellow and $-b^*$ blue). The total colour change (ΔE^*) was obtained based on the following equation: $\Delta E^*_{ab} = \sqrt{[(\Delta L^*)^2 + (\Delta a^*)^2 + (\Delta b^*)^2]}$ Where ΔL^* , Δa^* and Δb^* are the variations in the L^* , a^* and b^* coordinates for the treated and control samples [12-14].

4. Results

4.1. Petrographic study

The petrographic study revealed that the bed rock sample composed essentially of clay minerals, microcrystalline carbonates, iron oxides, rare amounts of microcrystalline quartz and opaque minerals. Carbonates occur as very fine-grained aggregates admixed with clay minerals. Iron oxides are disseminated in considerable amount in the sample and occur as very fine-grained aggregates admixed with clay minerals. Clay minerals occur as very fine-grained that constitute the matrix. Significant amount of microfossils and fossil fragments are filled by recrystallized carbonates, microcrystalline quartz, and it scattered in the matrix, fig. (3-a). Also, the petrographic study revealed that the studied support and plaster samples are composed of clay minerals, quartz and organic fibers, minor amounts of feldspars, biotite, rare pyroxene, epidote and glauconite. All these components are scattered in a matrix of clay minerals admixed with rare iron oxides and opaque minerals. Quartz occurs as fine to very fine-grained (sand size), sub-angular to angular grains scattered in the

matrix. The organic fibers of various sizes are elongated in the clay matrix. Biotite occurs as very fine to fine-grained, flaky crystals scattered in the sample. Clay minerals occur as very fine-grained aggregates that constitute the majority of the matrix. Feldspars occur as very fine to fine-grained, subhedral crystals, which can be observed in different parts of the samples, fig. (3-b & c).

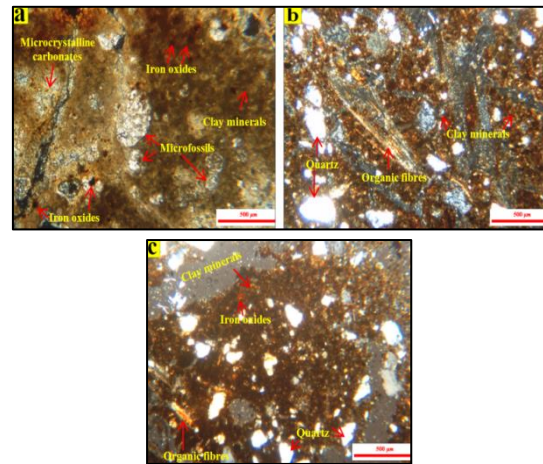


Figure (3) Shows microphotographs of the studied samples under plane polarized light; **a.** bed rock, **b.** mud brick support, **c.** mud plasters layers.

4.2. USB-digital microscope investigation

USB-digital microscope investigation revealed that the black pigment appears in a form of amorphous network, composed of very fine grains, shows a homogeneous distribution, and take black color with a slight blue hue, fig. (4-a). This suggested that black color was produced using carbon black of soot. It also showed that the white wash layer formed of homogenous fine grains and appears some voids distributed in the ground mass, which led to appearance of the straw, inform the preparatory layer below, fig. (4-b). The red pigment appears in a form of homogenous very thin layer, formed of fine to very fine grains and the straw appears in the preparatory layer below, due to poor coverage of the painted material, fig. (4-c). The pink pigment appears as a dense layer, formed of gradient-grained mixture of white and red grains and micro-cracks, fig. (4-d). It also illustrated that the

blue pigment consists of very coarse grains as layers dispersed in amorphous matrix. These results reflect the properties of the Egyptian blue, fig. (4-e). The green pigment appears as a thin layer, has many cracks, consists of a homogeneous coarse grain, with some yellow and blue grains distributed in the ground mass, in addition the loss of pigment in some places, which led to the appearance of the straw infrom the preparatory layer below, fig. (4-f). The yellow pigment appears intense color, as a compact, homogenous layer, has network of micro cracks and it is formed of different size particles which ranges from very fine to large grains, fig. (5-g). The white pigment formed of fine to very fine homogeneous grains that the same as the one utilized for the white wash layer but very thin and had a loos surface and micro cracks are spread in the ground mass, fig. (4-h). The network of micro cracks that appear in the painting layer, it is probably as a result to shrinkage of the clay minerals in the preparatory layers.

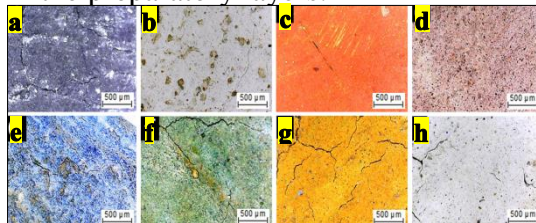


Figure (4) Shows digital microscope micrograph of studied pigment and wall painting layers ; **a.** black, **b.** white wash layer, **c.** red , **d.** pink, **e.** blue, **f.** green, **g.** yellow, **h.** white .

4.3. Morphological study

The morphological study was carried out by the scanning electron microscope and portable USB-digital microscope to reveal the deterioration aspects and surface properties of the samples that representing the layers of the studied wall paintings. SEM examination of the mother rock sample, fig. (5-a) revealed many cracks, the growth of salt crystals, some irregular pore spaces and channels. In addition, the sample exhibiting obvious lamination with irregular edges, which is thought to be one of the most crucial properties of clay minerals.

SEM examination of the mudbrick support sample fig. (5-b) showed presence of quartz, and chopped straw, which were added to the mixture of mud as bonding materials. Furthermore it showed the deterioration aspects, such as cracking, granular disintegration, cavities, fibers crash, and salt crystallization. SEM examination of the preparatory layers, fig. (5-c & d) revealed they were composed mainly of a mixture of clay, sand and chopped straw. Moreover, these layers are highly suffered from weakness in internal structure, loss of cohesive, where many cracks appear, and crash of the chopped straw. These results reflected the aggressive weathering to which the wall paintings in the tomb of Amenemhat (No 340) have been subjected.

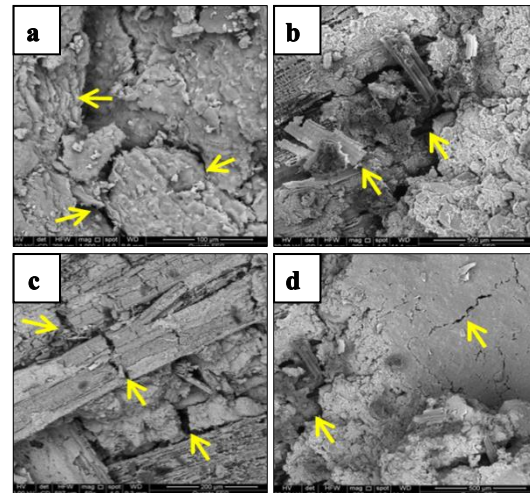


Figure (5) Shows SEM micrographs of the wall paintings layers; **a.** the mother rock, **b.** the mud brick support, **c.** & **d.** the preparatory layers.

4.4. Mineralogical & chemical compositions

XRD and EDX results are reported in the following points: **1)** the bedrock sample (Esna Shale), fig. (6-a) indicates that is consists of a mixture of montmorillonite $Al_2O_3 \cdot 4SiO_2 \cdot H_2O$, albite $NaAlSi_3O_8$, calcite $CaCO_3$, illite $(K,H_3O)(Al,Mg,Fe)_2(Si,Al)_4O_{10}[(OH)_2 \cdot (H_2O)]$ and anhydrite $CaSO_4$. EDS spectrum, tab. (2) confirmed this result, where the high beaks of Si, Al and O indicates the existence of aluminosilicate materials (e.g., clays) the main components of Esna shale. The beaks of Ca (16.60%), O (50.62%) and C (3.72%) indicate

the existence of calcite CaCO_3 . The peak related to Fe (3.81%) indicates the existence of iron oxides. The peaks of S (3.12 %) together with Ca implies the presence of anhydrite. The peaks of Na (0.93%) and chlorine (0.87%) proved the presence of halite mineral (NaCl) in the sample. **2)** the support sample, fig. (6-b) clarifies that is mainly consists of montmorillonite, albite, anorthite $\text{CaAl}_2\text{Si}_2\text{O}_8$, and quartz SiO_2 . EDX spectrum of the same sample, tab. (2) shows the presence of Si (25.26 %), Al (3.24%) and O (44.33%), Ca (2.76%), C (14.27%), Cl (0.63%), Na (0.42%) and Fe (8.67 %). The high peaks of Si, Al and O indicates the existence of aluminosilicate materials (e.g., clays), which are the main components of the mud bricks. The peaks of Na (0.42%) and Cl (0.63%) proved the presence of halite mineral (NaCl). XRD analysis of the plaster sample, fig. (6-c) indicates that is consists mainly of montmorillonite, albite, Kaolinite $\text{Al}_4(\text{Si}_4\text{O}_{10})(\text{OH})_8$, anorthite $\text{CaAl}_2\text{Si}_2\text{O}_8$, and quartz SiO_2 . Its EDS spectrum, tab. (2) confirmed this result, by presence of peaks related to Si (28.47%), Al (5.45%) and O (46.41%), the main components of aluminosilicates (clay minerals). XRD pattern of the yellow pigment, fig. (6-d) indicates that is consists mainly of goethite $\text{FeO}(\text{OH})$, quartz SiO_2 and traces of halite NaCl. Its EDS microanalysis, tab. (2) showing presence of C (4.34%), O (47.17%), sodium (3.19 %), Mg (0.93 %), Al (3.05 %), Si (10.08 %), Cl (4.15 %), K (0.39 %), Ca (22.74 %) and Fe (4.00 %). The peak related to iron indicates the existence of iron oxide (probably goethite, $\text{FeO}(\text{OH})$) as the possible material producing the yellow colour. The present of halite proved by the presence peaks of Cl and Na. XRD analysis of the red pigment, fig. (6-e) revealed that is consists mainly of hematite Fe_2O_3 and traces of quartz SiO_2 . Its EDS microanalysis, tab. (2) appears the presence of C (2.97 %), O (38.67 %), Na (3.19 %), Mg (0.44 %), Al (4.09 %), Si (9.90 %), Cl (3.67 %), K (0.45 %), Ca (12.69 %), Fe (23.93 %). The high peaks of iron, and oxygen clarified that iron oxides (probably hematite Fe_2O_3) is main material for red

color. The presence of Si and Al in EDX patterns of the yellow and red pigments samples implies the presence of aluminosilicate materials (e.g., clays) probably from the clay minerals associated with the red/yellow ochres and also often found in earth pigments [15]. The present of halite proved by the presence high peaks of Cl (4.15%) and Na (3.19%). XRD pattern of the blue pigment, fig. (6-f) revealed that is formed of Egyptian blue cuprorivaite $\text{CaCu}_2\text{Si}_4\text{O}_{10}$. EDS spectrum of the same sample, tab. (2) revealed it includes C (3.78 %), O (38.63 %), S (0.52 %), Mg (0.87 %), Al (1.06 %), Si (22.86 %), Cl (0.94 %), K (0.50 %), Ca (14.90 %), Fe (0.93 %), and Cu (15.00 %). These data confirmed that the blue pigment is mainly formed of cuprorivaite $\text{CaCu}_2\text{Si}_4\text{O}_{10}$ (Egyptian blue); where the atomic percentage ratio of Ca (14.90 %), Si (22.86 %), and Cu (15.00 %) are in agreement with the chemical formula of cuprorivaite or calcium-copper tetrasilicate. The peaks of Na (3.19%) and Cl (3.67%) proved the presence of halite mineral (NaCl) in the sample. XRD analysis of the pink color, fig. (6-g) indicates that is consists mainly of gypsum $\text{CaSO}_4 \cdot 2\text{H}_2\text{O}$, calcite CaCO_3 , and hematite Fe_2O_3 . EDS analysis, tab. (2) confirmed the presence of iron oxides (probably hematite Fe_2O_3) by the presence of the high peaks of iron (4.11 %). Presence of calcium (26.72 %), oxygen (57.82 %) and sulfur (4.25 %) peaks implies the presence of gypsum. The peaks related to Ca (26.72%), C (3.21%) and O (47.82%) indicates the existence of calcite CaCO_3 . This result confirms that the ancient Egyptian artist obtained the pink color by mixing calcium sulfate with calcium carbonate and hematite. The presence of halite was proved through the peaks of chlorine (0.99%) and sodium (0.66%). XRD analysis showed that the white wash sample, fig. (6-h) consists of gypsum $\text{CaSO}_4 \cdot 2\text{H}_2\text{O}$ as a major constituent, and anhydrite CaSO_4 as a minor constituent. The elemental analysis of the same sample, tab. (2) confirmed this result by the presence of the high peaks of O (43.65 %), S (21.82 %), and Ca (33.70 %). EDS spectrum of the black pigment, tab.

(2) revealed that is consists of C (8.75), O (42.82 %), Na (0.70 %), Al (2,55 %), Si (12.81 %), Cl (6.65 %), Ca (18.52 %) and Fe (7.20 %). The high beaks of C (8.75 %) confirmed that the carbon is the most probable as a black color. EDS spectrum of the green pigment, tab. (2) demonstrated

that is formed of Cu (16.91 %), C (29.73 %), O (29.08 %), Ca (16.60 %), Si (1.43 %), Na (0.70 %), Mg (0.25 %), Al (0.61 %), and Cl (4.70 %). The high beaks of C (23.93 %) and Cu (16.91) that probably suggests the use of malachite $Cu_2(CO_3)(OH)_2$ for green pigment.

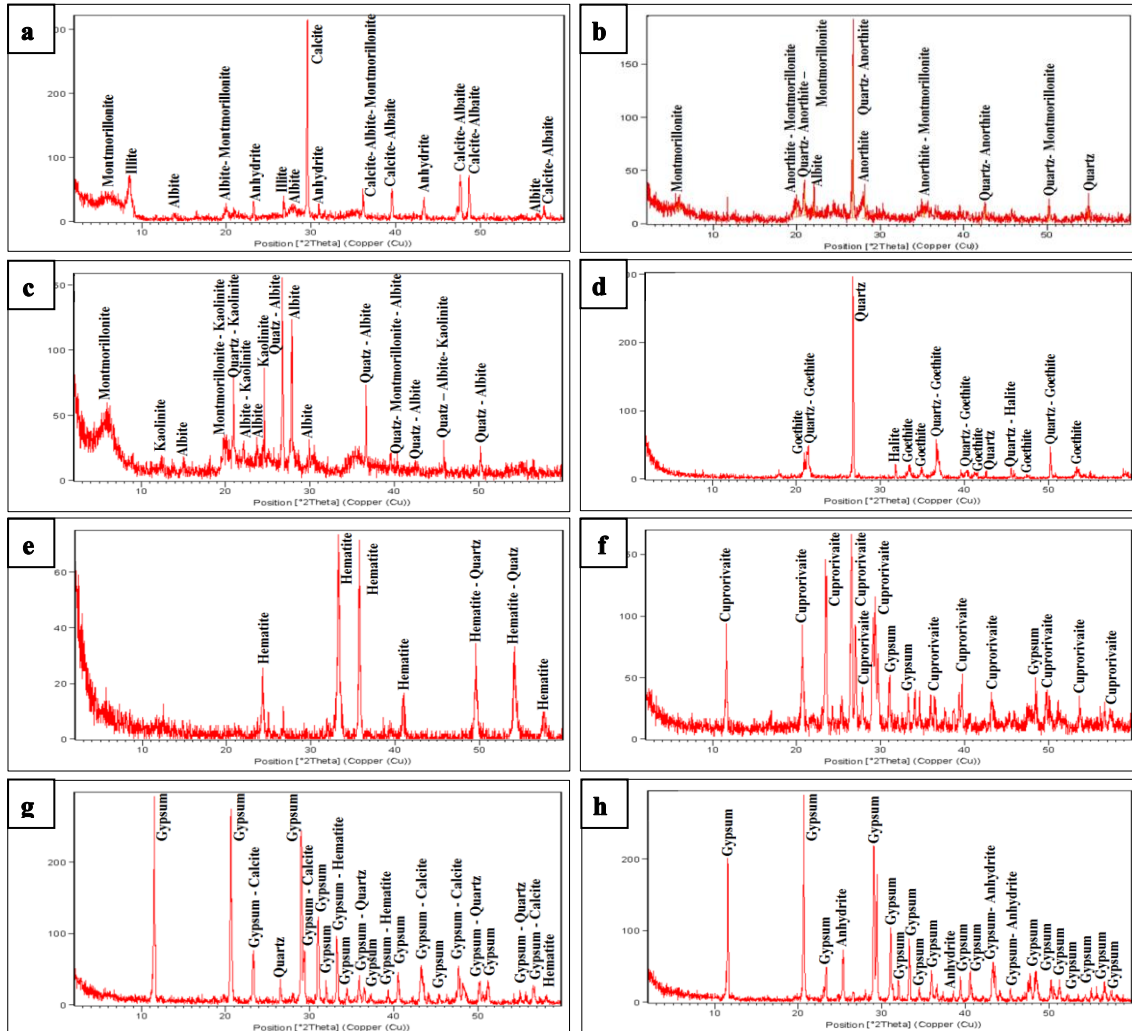


Figure (6) Shows XRD patterns of **a.** bedrock, **b.** support, **c.** plaster layer, **d.** yellow pigment, **e.** red pigment, **f.** blue pigment, **g.** pink pigment, **h.** white wash layer.

Table (2) summarized the EDX Microanalysis (Atomic w.t. %) of the studied samples.

Elements	Samples										
	Bedrock	Support	Plaster	Yellow Pigment	Red Pigment	Blue Pigment	pink Pigment	White Wash	Black Pigment	green pigment	
Wt %											
C	3.72	14.27	7.11	4.34	2.97	3.68	3.21	-	8.75	29.73	
O	50.62	44.33	46.41	47.17	38.67	38.63	47.82	43.65	42.82	29.08	
Na	0.93	0.42	0.52	3.19	3.19	0.52	0.66	-	0.70	0.70	
Mg	-	-	-	0.93	0.44	0.87	-	-	-	0.25	
Al	3.09	3.24	5.45	3.05	4.09	1.06	-	-	2.55	0.61	
Si	17.24	25.26	28.47	10.08	9.90	22.86	12.23	0.83	12.81	1.43	
S	3.12	0.40	0.37	-	-	-	-	21.82	-	-	
Cl	0.87	0.63	0.63	4.15	3.67	0.94	0.99	-	6.65	4.70	
K	-	-	-	0.39	0.45	0.50	-	-	-	-	
Ca	16.60	2.76	2.18	22.74	12.69	14.90	26.72	33.70	18.52	16.60	
Fe	3.81	8.67	8,86	3.96	23.93	0.93	4.11	-	7.20	-	
Cu	-	-	-	-	-	15.00	-	-	-	16.91	

4.5. FTIR results

The results of FTIR analysis to the archaeological red sample, fig. (7) showed the signature of stretching band of (OH) group at 3286.2 cm^{-1} , the bending band of (C-H) group at 1415.5 cm^{-1} , and stretching band of C-O group at 1033.7 cm^{-1} . From these results, so Arabic gum is highly recommended to be the organic binder of mural painting in the tomb of Amenemhat (No. 340).

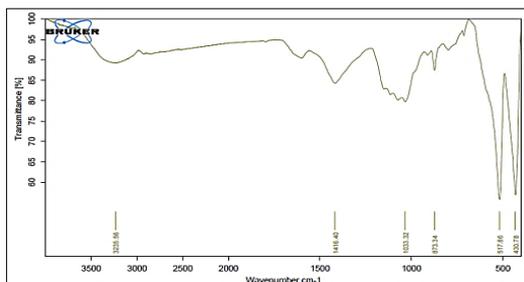


Figure (7) Shows FTIR pattern of red painted archaeological sample

4.6. Evaluation of the samples after treatment

4.6.1. Scanning electron microscope (SEM)

Morphological characterization of the treated samples was performed by using SEM to examine and evaluate the ability of the consolidation materials used in this study to consolidate the studied samples of painting layer and mud plaster. From SEM micrographs of the untreated and treated samples, it can be noted that **1**) The untreated sample of painting layer appeared to be very fragile and has many wide pores and fine cracks, fig. (8-a). **2**) The sample of painting layer treated with Klucel G 1% in ethyl alcohol, fig. (8-b) illustrated that the consolidation product has achieved a homogenous distribution on the surface, filling micro cracks and the pores without blocking them and has the excellent ability to bind the particles. **3**) The sample of painting layer treated with Plexisol P550 2% in acetone, fig. (8-c) shows that the consolidation product coated the sample with a thin film caused to blocking pores. **4**) The sample of painting layer treated with paraloid B72 3% in acetone, fig. (8-d) appears that the consolidation product covered the sample with dense polymeric coat led to blocking

pores of the surface. **5**) The untreated sample of mud plaster has a weak internal structure, brittle, loses cohesion between its grains and filled with fine cracks as shown in SEM photomicrograph, fig. (9-a). **6**) The products of Bio Estel and Estel 1100 are succeeded in consolidate the mud plaster samples, as both of them achieved a good distribution on the surface, filled the pores without blocking them and forming a homogenous polymeric networks caused to improving the bonding between the grains as shown in SEM micrographs, fig. (9-b & c). **7**) The product of Wacker OH 100 achieved a good distribution on the surface of mud plaster sample, filled the small pores and formed a superficial layer full of micro cracks in some places. In addition, it failed in filled the wide pores and improving the binding between the large grains as shown in SEM photomicrographs, fig. (9-d).

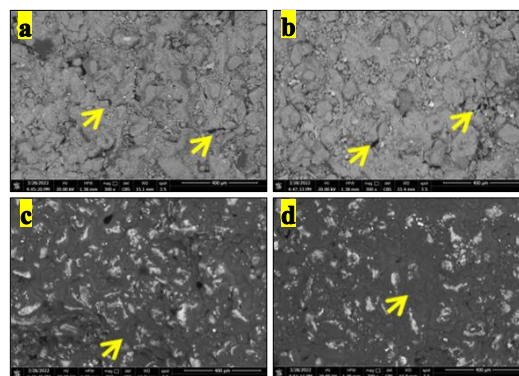


Figure (8) Shows SEM micrographs of treated and untreated samples of painted layer with 300x; **a.** untreated sample, treated sample by **b.** Klucel G, **c.** Plexitol, **d.** paraloid B72.

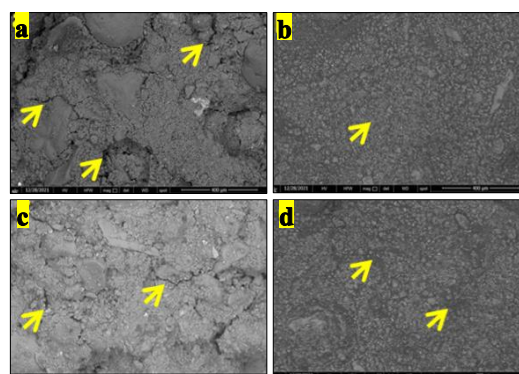


Figure (9) Shows SEM micrographs of treated and untreated samples of mud plaster with 300x; **a.** untreated sample, treated sample by **b.** Bio Estel, **c.** Wacker OH 100 **d.** Estel 1000.

4.6.2. Colour alteration

According to guidelines for conservation purposes of historical or monumental surfaces, the ΔE value must be <5 [16-18]. The ΔE values obtained from the chromatic measurements of the treated and untreated samples by UV-3101PC spectrophotometer are listed in tab. (3).

Table (3) Results of the chromatic measurements of the treated and untreated samples

Samples		L*	a*	b*	ΔE^*
White	Untreated sample	94.69	0.47	3.79	-
	Treated with Klücel G	93.41	0.91	4.51	1.53
	Treated with Paraloid B72	87.06	1.69	8.27	8.93
Black	Treated with Plexisol 550p	87.45	2.12	6.19	7.80
	Untreated sample	33.61	-0.26	-1.06	-
	Treated with Klücel G	32.97	0.29	-1.17	0.85
Red	Treated with Paraloid B72	23.74	0.32	-0.33	9.91
	Treated with Plexisol 550p	25.19	0.30	-0.21	8.48
	Untreated sample	47.48	12.54	5.35	-
Yellow	Treated with Klücel G	46.11	11.31	5.06	1.86
	Treated with Paraloid B72	38.91	12.89	7.12	8.75
	Treated with Plexisol 550p	38.13	14.81	7.17	7.13
Blue	Untreated sample	66.35	11.60	31.25	-
	Treated with Klücel G	65.15	11.93	31.79	1.36
	Treated with Paraloid B72	60.01	13.84	38.20	9.67
Green	Treated with Plexisol 550p	58.21	14.72	31.12	8.72
	Untreated sample	67.55	-4.54	-5.77	-
	Treated with Klücel G	66.13	-4.78	-6.25	1.52
Mud plaster	Treated with Paraloid B72	60.24	-7.91	-9.52	8.88
	Treated with Plexisol 550p	61.97	-7.02	-8.08	6.53
	Untreated sample	65.89	-10.77	-1.45	-
Mud plaster	Treated with Klücel G	64.57	-9.79	-1.98	1.73
	Treated with Paraloid B72	59.11	-15.53	-3.16	8.49
	Treated with Plexisol 550p	60.29	-14.53	-2.99	6.92
Mud plaster	Untreated sample	51.41	3.88	10.59	-
	Treated with Wacker OH 100	59.63	7.20	15.65	8.57
	Treated with Bio Estel	53.33	5.85	12.25	3.21
Treated with Estel 1100	55.37	6.37	14.34	5.99	

4.6.3. Evaluation of the prepared mortars

4.6.3.1. Aesthetical properties

The aesthetical compatibility between the archaeological mud plaster and prepared mud mortars was determined by colourimetric measurements, tab. (4).

Table. (3) Chromatic alterations between the prepared mud mortars and archaeological plaster.

Samples	L*	a*	b*	ΔE^*
Archaeological mud plaster	51.41	3.88	10.59	-
Mortar (1)	50.22	3.97	10.64	1.02
Mortar (2)	59.96	2.42	8.37	8.95
Mortar (3)	46.23	2.11	7.47	6.30

4.6.3.2. The visual appraisal

The visual appraisal of the prepared mortar samples, fig. (9) after drying and setting revealed that the mortar (M1) has good cohesion, and homogeneous texture with no cracks, and it is compatible in color with the original mud plaster. Also, mortar (M2) has good cohesion, has rough texture with no cracks, dark color, which is incompatible with the original mud plaster. In addition, mortar (M3) is too weak, fragile, has rough texture with no cracks and highly white in color, which is incompatible with the original mud plaster.

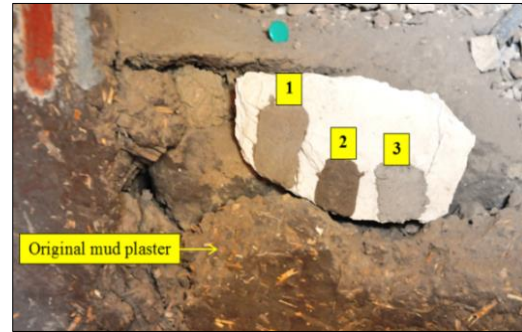


Figure (9) Shows general appearance of the prepared mortars samples.

5. Discussion

Based on the above examinations and analyses results, it is evident that the ancient Egyptian artist used the traditional technique which is used inside the rock tombs for preparing the wall paintings at the tomb of Amenemhat (No. 340), including its stratigraphic sequence, fig. (10).

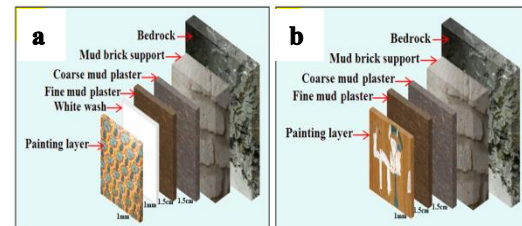


Figure (10) Shows **a.** the stratigraphy sequence of mural painting of the tomb ceiling, **b.** the stratigraphy sequence of mural painting of the tomb walls.

Where in the first, the tomb was dug into the Esna Shale formation in the eastern hill of Deir el-Madina, through a roughly hewn passage that continued until was reached needed length of the tomb. Due to the fragile nature of the bedrock, the hewn tomb has been lined up from the inside with mud bricks walls to give it a desired shape (rectangular with barrel-vaulted ceiling). The mud brick walls were later coated with two different preparatory layers of mud: a coarse one on the mud bricks, then a finer one for painting. The coarse layer has (3: 3.5 cm) thickness and consists of mud mixed with chopped straw and coarse grains of sand. The fine layer has (1:1.5 cm) thickness and consists of mud mixed with straw and fine grains of

sand. It's worth mentioning that the oldest mural painted tomb in Egypt on a mud brick support and mud plaster layers that has been found to date, is the tomb 100 in Herankopolis at Upper Egypt, dating to the Naqaada II/Gerzean period (c.3200 BC) [19]. The use of mud plaster has been attested since the pre dynastic and the early dynastic periods [20]. It is the most abundant in the Theban tombs (perhaps for availability of natural raw materials, its ease of preparation, and lack of cost) [21]. For decorate the prepared walls, the artist painted the background directly on the mud plaster using yellow pigment of goethite $\text{FeO}(\text{OH})$, as a very thin monolayer, as appears on the north and east walls, fig. (3-a:c). The preparatory drawing was applied by white pigment on the yellow background, as appears in the unfinished north side of the eastern wall. For coloring the figures, the white pigment composed of gypsum $\text{CaSO}_4 \cdot 2\text{H}_2\text{O}$ and anhydrite CaSO_4 was used to paint the clothing, offerings, and objects. Calcium sulfate pigments are well recognized in ancient Egyptian art of all periods, but no exact date of its first application and it probably was used from the 5th dynasty till the Roman time. It was reported that the most commonly used as a white pigment in ancient Egypt are anhydrite (CaSO_4), gypsum ($\text{CaSO}_4 \cdot 2\text{H}_2\text{O}$) and calcium sulfate semi hydrate ($\text{CaSO}_4 \cdot 0.5\text{H}_2\text{O}$) [22]. Red pigment of hematite Fe_2O_3 was used to paint the men skin tones. The hematite (Fe_2O_3) is the most commonly used red pigments in ancient Egypt starting from the pre-dynastic period and it has been recorded in all works of art over all periods. In Egypt, it is naturally occur in the Oases of the Western desert and near Aswan, it is prepared by washing, levitating and grinding [23-29]. The yellow pigment of goethite $\text{FeO}(\text{OH})$ was used to paint the women skin tones. Goethite was the main source of yellow colour in ancient Egypt and it was widely used from pre-dynastic times to the Roman period with no interruption. It is naturally occurring

earth pigments formed from either direct weathering of deposits that are rich in iron or concentrated iron from underlying bedrocks. In Egypt it is naturally occurs around Aswan and in the oasis of the western desert [30,31]. The black pigment of carbon soot (C) was used to paint the hair, details and the outlines of the figures. Soot or lampblack is amorphous carbon produced by burning oils and resins especially rosin and candle wax. It is most commonly used in Egyptian murals and cannot be distinguished from the XRD pattern [32,33]. The blue pigment of Egyptian blue (cuprorivite $\text{CaCu}_2 \text{Si}_4\text{O}_{10}$) was used to paint ornaments and accessories. Egyptian blue is the first man made synthetic pigment. In Egypt the earliest known uses of Egyptian blue are from the 4th dynasty (c.2613-2494 BC) and it was used up to the Roman period. The secret of its manufacture was lost after downfall of the Roman Empire only to be re discovered in the nineteenth century. This synthetic pigment was making by mixing calcium salt (carbonate, sulphate or hydroxide), a copper compound (oxide or malachite), sand (silica) and an alkali flux (sources of alkali could either have been natron from areas such as Wadi Natrun and ElKab, or soda-rich plant ashes) [34]. This mixture then is heated to a temperature between 850-1000 C to produce a colored glass or frit and ground it to powder for using [35-38]. The green pigment of malachite $\text{Cu}_2(\text{CO}_3) \cdot (\text{OH})_2$ was used to paint the plant elements and skin tones of gods. Malachite is a green basic copper carbonate mineral with composition $\text{Cu}_2\text{CO}_3(\text{OH})_2$. Its name is derived from a Greek meaning 'mallow' and refers to its leaf green colour. It was used in Egypt for eye-paint as early as pre-dynastic times and has been found on tomb paintings from the 4th dynasty. In Egypt, it occurs on Sinai and in the Eastern desert. Its characteristics are very similar to azurite and aggregates of the two minerals together are frequently found. It was prepared for use as a pigment by crushing, grinding, washing and levigating [39,40]. In addi-

ion, the pink pigment composed of gypsum $\text{CaSO}_4 \cdot 2\text{H}_2\text{O}$, calcite CaCO_3 and hematite was used for painted the pottery. All of used pigments were prepared for the paint by mixed with Arabic gum as organic binder. Vaulted ceiling presents a different style to application murals in the studied tomb. It is clear that the yellow background for the figures was execute over a whitewash layer composed of gypsum $\text{CaSO}_4 \cdot 2\text{H}_2\text{O}$ and anhydrite CaSO_4 , that was applied directly up on the mud preparatory layer. This explains why the vaulted ceiling's yellow is more vivid than that of the other walls. Gypsum was widely used in ancient Egyptian times as a white wash (thin layer or layers) in order to treat irregularities and smooth the surface for drawing and painting, due to its cheapness, widespread availability and religious significance as a symbol of purity and cleanliness [40-43]. The presence of preparatory drawing and the corrections of the decoration (drawings and texts) in addition no outline around the figures in the north and east walls are reflecting that the artists probably did not have time to finish decorating the tomb. It seems that the author of this decor is the son of the owner "Sennefer". The faults and clumsiness in the inscriptions of the decoration prove his lack of experience and his illiteracy. Where texts were copied and pasted without understanding their meaning [44]. Based on the results of analytical methods and visual observations, it was clear that the studied mural paintings are suffered from the influence of physicochemical, biological and human deterioration factors, which appeared by many deterioration aspects such as the tiny holes of insects. Where the components of mural layers (mud brick and mud plaster) are provides a suitable food source and environment for insects to dwell, especially presence of the organic component of chopped straw fibers [45]. Also, the wasps' saliva used to create the wild wasps' nests, caused efflorescence on the surface of murals and chromatic alterations, as a result to

mixing with the components of the surface layer. Moreover, due to strong adhesion of wild wasps' nests on the weak mural layers, it requires a lot of attention to removal [46]. In addition, the accumulation of dust on the surface of mural paintings, this led to the blurring of the aesthetic appearance. It needs to be cleaned by safe methods and materials [47]. The loss of the paint layer (powder) in some areas may be due to the loss of pigment cohesion, as the Arabic gum binder decomposes, brittle and dry by exposure to high temperatures [48]. Furthermore, the voluntary losing of the paint layer in all the eyes of the characters. In many beliefs the eyes had a power. For this propos it is possible that the Copts occupied the tomb, modified its function and reused [49]. The cracks, detachments, bulges and large structural gaps in the studied wall paintings are probably caused by some chemical reactions that cause different pressures between the bedrock and mural paintings. For instance the bedrock of Esna shale Formation is susceptible to swelling after absorbing moisture from the flash floods at the study area, such as the floods in 1994 [50]. The pressures resulted from swelling of clay minerals in the bedrock directly affect the adhesion forces of the mural painting layers (mud brick support and mud plaster) [51-55]. Another problem with the bedrock is the presence of different evaporative minerals such as halite and sulphate minerals, which damage the mural paintings due to volume changes based on the heat difference and evaporation of water rates. Halite is hygroscopic, capable of retaining adsorbed humidity in the masonry and highly detrimental when it recrystallizes between the layers (sub florescence) as a result to temperature changes, where it appears volumetric expansion with higher temperature. That volumetric expansion creating mechanical pressure between the bedrock and the mural paintings leads to cracking; paint flaking, disintegration, increases deterioration rates and decreasing the adhesion forces between the support and the plaster layer and or the painting layers to com-

pleted loss in paint. Also, the presence of sulphates group in the bedrock causes problems, where it expands due to changes from the anhydride to the hydrated state and creates pressures between the bedrock and the mural paintings leads to the same damages that resulting by swelling pressure of clay and the crystallization pressure of halite, Also, some cracks in the ground layers are associated to the conversion of gypsum into anhydrite. [51, 52,56-59]. From the foregoing, it is clear that the consolidation, cleaning, and filling of cracks and gaps are the main treatment procedures of studied wall paintings. This helps to reveal their aesthetic and artistic values, recover their strength, increase their durability, and enables periodic conservation. Therefore, three widely used products for consolidation of painted materials (Klucel G 1%, Plexisol 550p 2% and Paraloid B72 3%) were selected and evaluated to use the most suitable product to consolidate the painting layer. Moreover, three products of silicon-based polymers (Estel 1100, Bio Estel and Wacker OH 100) were selected and evaluated in order to determine which would be the best choice for consolidate the mud plaster layer. The SEM examination of the experimental samples of the pigments demonstrated that the product of (Klucel G1%) has achieved a homogenous distribution on the surface of treated sample, filling micro cracks and the pores without blocking them and has the excellent ability to bind the particles. This may be related to the lower molecular weight grades to the Hydroxypropyl cellulose (Klucel G) [60]. While the product of Plexisol 550p 2% coated the samples with a thin film caused to blocking pores. This process may be related to porosity and surface homogeneity of the sample in addition the nature, concentration and viscosity of the polymer [61,62]. Also, Paraloid B72 3% covered the sample with dense polymeric network led to blocking pores of the surface. This process may be related to the large size of Paraloid B-72 molecules, density, high viscosity of the solution, the

type of used solvent in preparation and its partial dissolution in organic solvent. It is certainly that Paraloid B-72 polymer has a substantially lower penetration rate than pure solvent, even at low concentrations [63,64]. Furthermore, SEM examination of the mud plaster experimental Bio Estel and Estel 1100 were achieved a good spread on the surface, filled the pores without blocking them, formed homogenous polymeric networks and achieved good adhesion between deteriorated areas and conserved areas. This can be attributed to the compatibility and homogeneity between the chemical composition of mud plaster and used silicone polymers. Moreover, the product of Wacker OH 100 is not the best for consolidation process compared to the studied products, as it achieved a good distribution on the surface, filled the small pores between the grains, formed a superficial layer full of micro cracks in some places, failed in filled the wide pores and improving the binding between the large grains. The tendency to crack during shrinkage and drying is a serious disadvantage of alkoxysilane products especially Wacker OH 100 [65]. The results of colourimetric analysis demonstrated that the consolidation product (Klucel G1%) did not cause any effect on the color and the general appearance of the treated pigments samples (white, black, red, yellow, blue and green), as it achieved the total colour change value less than the threshold values of guidelines for conservation. Moreover, the products of Paraloid B72 and Plexisol 550p are failed to conserve the nature color of treated pigment samples, as they recorded highest values of ΔE , exceeding guidelines values of conservation purposes. This can be attributed to the photodegradation of acrylic polymers as a result to the formation of conjugated double bonds systems [66]. In addition, mud plaster samples treated by Bio Estel achieved the best results, where record lowest value of total colour change <5 . But the product of Estel 1100 caused a slight change in the colour of treated mud plaster samples. Whilst Wacker OH 100

caused a significant color alteration of treated mud plaster samples, where it achieved the highest value of total color change, exceeding guidelines values of conservation purposes. This can be attributed to the type of solvent used in the preparation of the polymer. According to the above results of the experimental studies of consolidation treatment, it is clear that the product of Klucel G 1% is the most suitable product to use for consolidation the painted layer. This confirms the results of recent studies [67]. Moreover, the product of Bio Estel is the most suitable product to use for consolidation the mud plaster layers of the wall paintings at the tomb of Amenemhat (No 340). Also, three types of prepared mortars were studied and comparatively to select the best one for filling gaps and cracks in the studied wall paintings. To achieve the aesthetical compatibility between the prepared mortars and the preparatory layers of mural paintings, the same local natural materials that were used in the past to be carried out the preparatory layers in the studied murals have been used, which revealed by the methods of examination and analysis. According to the results of the colourimetric analysis, the prepared mortar (M1) is the most suitable mortar to use for filling cracks, joints and gaps in the wall paintings at the tomb of Amenemhat (No 340), as it has the most compatible colour with the studied archaeological plaster, where it achieved total colour difference value less than the threshold values of guidelines for conservation. Visual examination confirmed this result; besides it possess a homogeneous texture with no cracks and good cohesion. This can be attributed to that the compositional proportions of the prepared mortar (M1) correspond to the compositional proportions of the studied archaeological preparatory layers in a large percentage. In addition, the prepared mortars (M2) and (M3) are incompatible in appearances with the studied archaeological plaster, as they achieved total colour differences values >5 . This can be attributed to the inco-

mpatibility between the proportions and components of prepared mortars (M2) and (M3) with the proportions and components of archaeological plaster.

6. Conservation Procedures

Based on the above mentioned studies, the studied wall paintings were treated according to the following criteria.

6.1. Pre-consolidation

Firstly; temporary strips of Japanese paper were applied using Klucel 3%, to secure the weak parts of mud plaster and prevent it from collapsing during the treatment process.

6.2. Mechanical cleaning

It has been tested multiple cleaning tools to determine the best one to use for mechanical cleaning. The results of the test confirmed that the appropriate tools are soft brushes with white hair, wishabs, bamboo sticks, scalpels, spatulas and manual air pump to low air pressure. Then, surface deposits were carefully removed from the surface of the wall paintings after they had undergone pre-consolidation. Where, the soft brushes and air pump were used to remove the dust from of mural paintings. While scalpels, small spatulas, wishabs, and bamboo sticks were used to remove deposits and wasps' nests, fig. (11-a).

6.3. Re-adhesion of partly detached and flaking paints

To treatment the partly detached and flaking paints of the wall painting, we injected Klucel G 3% in the small voids between the painting layer and mud plaster layer using a thin syringe. Then, we put the polyethylene sheet over these areas and pressed on it lightly with small spatula or our fingers, until attached well to the mud plaster layer.

6.4. Consolidation treatment

According to the results of experimental study, Klucel G 1% was used to consolidate the weak painting layer. The consolidation product of Bio Estel was heavily applied on parts of the mud plaster which the painting layer has fallen of

and the weak edges of the mud plaster layer in the missing parts, in order to improve bonding between grains and organic fibers. The consolidation process was applied using soft, white-bristle brushes, in several stages at successive times, to allow the consolidation products to diffuse and penetrate deeply into the layers, fig. (11-b).

6.5. gaps and missing parts

The goal of this treatment is to conserve the remaining parts of wall paintings and prevent it from collapsing in the future [68]. The first step is to consolidate the outer edges of the mud plaster around the gaps and missing parts using Bio Estel, to prevent fragmentation and crumbling during the application of the new mortar. Then, we filled the missing parts with prepared mud mortar (M1), as it is compatible in color and texture with the original plaster, according to the results of experimental studies. The mortar was applied and finished it using fine spatulas. In order to treat the gap in the west wall, we removing fragments of stones and mud bricks from inside the gap that was filled during a previous intervention without mortar. Then, the mud bricks were stacked inside the gap again and the mud mortar was applied between them and on all sides, to achieve a good bonding. In the end, the prepared mortar (M1) was used to fill the gap surface from inside to outside as mono layer and finishing it using fine spatulas, fig. (11-c & d).

6.6. Detachment and cracks injections

There were many areas where the mud plaster had partly detached from the support, which causes a void to form between them. To treatment these parts, the grouting material P.L.M- AL was used. It is a mixture of neutral lime with hydraulic additives and selected inert additives free from salts .It is widely used for the consolidation of detached frescoes and plasters from the mural substrate, to which it gives new clinginess characteristics without

increasing the weight of the supporting structure. The treatment process was performed as follows: **1)** Identify injection holes, this ensures that the grouting material is well distributed and reaches the largest possible area. **2)** Close the out edges of the detachment parts and any holes or cracks nearby using prepared mud mortar (M1), to prevent leakage of the grouting material during injection, fig. (11-e & f). **3)** Injection 1 syringe of alcohol in the injection hole in order to clean the dust and prepare the hole for the injection of the grouting material. **4)** Starting the injection process using P.L. M - AL, from the lower level to the higher level, with full monitoring and counting the number of injections in each part. **5)** After completion of the grouting process, the plastic tubes or syringe are removed from the injection hole, and closed the hole using prepared mud mortar (M1), fig. (11-g & h). [69].



Figure (11) Shows the stages of conservation; **a.** mechanical cleaning, **b.** consolidation, **c.** the gap during treatment, **d.** the gap after treatment, **e.** the crack before the treatment, **f.** the crack after treatment, **g.** & **h.** treatment of the detachments

7. Conclusion

Based on the visual appraisal, microscopic examination and analytical study it is evident that the ancient Egyptian artist was used the traditional technique (tempera) for preparing

the wall paintings in the Theban tomb (No. 340) at Deir el-Madina necropolis, western Thebes, Luxor, Egypt. The stratigraphic of studied wall paintings are forming of mud brick support, mud plaster as two layers (a coarse, and a finer), gypsum white wash (only on the ceiling) and painting layer formed of different pigments mixed with Arabic gum; Egyptian blue (blue color), hematite (red color), goethite (yellow color), gypsum (white color), malachite (green color) and carbon (for black color). These wall paintings have been exposed to many endogenous and exogenous deterioration factors. The endogenous factors include the fragile nature of the bedrock (Esna shale) and weak materials used in the wall paintings, such as the mud-brick support and mud plaster layers. The exogenous factors represented by the physicochemical, biological and human deterioration factors. Superficial strange deposits of wild wasps' nests, paint loss, holes, gaps, cracks, micro-cracks, hairline cracks, salts, detachments, and bulges were the dominant damage aspects at the studied mural paintings. Due to the high fragility of the studied mural paintings, the processes of consolidation and filling gaps and cracks were represented the most important challenges in the treatment. The results of experimental study showed that the product of (Klucel G) has high efficiency in the consolidation of the weak painting layer, with preserve the general appearance of the treated samples of pigments. Also, the product of Bio Estel it characterized by higher consolidation effect, in addition to not causing aesthetical changes of the mud plaster layer. Moreover; the experimental study of the prepared mortars revealed that the mortar (M1) it suitable for filling gaps and joints in the mural paintings, as it has good cohesion, homogeneous texture with no cracks, and much more suitable and matching in color with the original mud plaster. The conservation methodology were successfully carried out to treatment the studied mural paintings, which include multiple processes. The first of them is a pre-consolidation process by fixing strips of Japanese paper using Klucell 3%, to secure the weak parts of mud plaster. The mechanical cleaning using the appropriate tools was successfully to remove the surface deposits and wasps' nests from the mural paintings. Klucell G 3% was successfully used to Re-adhesion of partly detached and flaking paints. The consolidation treatment was carried out depending on the results of experimental study, where we decided to use Klucel G 1% to consolidate the weak painted layer, and to use Bio Estel for consolidate the fragile mud plaster layers by brushes. Also filling gaps and missing parts were successfully employed using mo-

rtar (1) by fine spatulas. Treatment of detachment parts and cracks it was successfully carried out by injection the grouting material of P.L.M to attach the separated plaster.

Acknowledgements

The authors would like to thank Prof. Dr. Cedric Larcher (Head of the French mission in Deir el-Medina archaeological site) and Manon Lefevre (Conservation responsible at Deir el-Medina archaeological site), for their assistance during the study and conservation of the mural paintings in the tomb of Amenemhat (No 340).

Reference

- [1] McDowell, A. (1999). *Village life in ancient Egypt: Laundry lists and love songs*. Oxford: Oxford Univ. Press, UK.
- [2] Exell, K. (2007). *A social and historical interpretation of Ramesside period votive stelae*, Ph.D., Vol. 1, Archaeology dept., Durham Univ., UK.
- [3] Andreu, G. (2002). *Les artistes de pharaon: Deir el-Medineh et la vallee des Rois*, Editions de la Reunion des Musees Nationaux, Paris.
- [4] Jaana, T. (2011). Deir el-Medina (Development), *UCLA*, Vol. 1 (1), pp. 1-15.
- [5] Cherpion, N. (1999). *Deux tombes de la XVIIIe dynastie à Deir el-Medina n° 340 (Amenemhat) et 354 (anonyme)*, MIFAO, Le Caire.
- [6] Aubry, M., Dupuis, C, Berggren, W., et al. (2016). The role of geoarchaeology in the preservation and management of the Theban necropolis, West bank, Egypt, *Proceedings of the Yorkshire Geological Society*, Vol. 61, pp. 134-147.
- [7] Aubry, M., Berggren, W., Dupuis, C., et al. (2009). Pharaonic necrostratigraphy: A review of geological and archeological studies in the Theban necropolis, Luxor, West bank, Egypt, *Terra Nova*, Vol. 21 (4), pp. 237-256

- [8] Dupuis, C., Aubry, M., King, C., et al. (2011). Genesis and geometry of titled blocks in the Theban hills, near Luxor (Upper Egypt), *J. of African Earth Sciences*, Vol. 61, pp. 245-267.
- [9] Helmi, F. & Hefni, Y. (2016). Using nanocomposites in the consolidation and protection of sandstone, *IJCS*, Vol. 7 (1), pp. 29-40.
- [10] Aldosari, M., Darwish, S., Adam, M., et al. (2019). Evaluation of preventive performance of kaolin and calcium hydroxide nanocomposites in strengthening the outdoor carved limestone, *Archaeological and Anthropological Sciences*, Vol. 11, pp. 3389-3405.
- [11] Baderi, N. & Ashry, A. (2016). The caning of the Isis temple's mural paintings in upper Egypt using zinc oxide nanoparticles and non-ionic detergent, *IJCS*, Vol. 7 (2), pp. 443-458.
- [12] CIE S014-4/E. (2007). *Colorimetry, CIE 1976 L*, a*, b* colour space*, Part 4, Commission Internationale de l'éclairage, CIE Central Bureau, Vienna.
- [13] Darwish, S. (2013). Evaluation of the effectiveness of some consolidants used for the Treatment of the XIXTH century Egyptian cemetery wall painting, *IJCS*, Vol. 4 (4), pp. 413-422.
- [14] Abdelaal, S. & Sandu, I., (2019). Assessment of protease in cleaning of bat blood patches from ancient Egyptian wall paintings and surface inscriptions, *IJCS*, Vol. 10 (3), pp. 459-474.
- [15] Afifi, H., Hassan, R., Abd-EL-Fattah, M., et al. (2020). Spectroscopic characterization of preparation, pigment and binding media of archaeological cartonnage from Lisht, Egypt, *Scientific Culture*, Vol. 6 (1), doi: 10.5281/zenodo.3483983
- [16] Francesca, P., Antonella, P., Alessandra, T., et al. (2018). TiO₂ nanocrystal based coatings for the protection of architectural stone: The effect of solvents in the spray coating application for a self-cleaning surface, *Coatings*, Vol. 8, doi: 10.3390/coatings8100356.
- [17] Giovanni, B. & Placido, M. (2015) Preservation of historical stone surfaces by TiO₂ nanocoatings, *Coatings*, Vol. 5 (2), pp. 222-231.
- [18] NORMAL. (2017). Misura colorimetrica strumentale di superfici opache, http://www.architettilroma.it/fpdb/conultabc/File/ConsultaBC/Lessic_NorMal-Santopuoli.pdf (2-8-2022).
- [19] Hanna, M. (2009). *Problems of preservation of mural paintings in the Theban necropolis, A pilot study on the Theban tomb 14 using 3D scanning techniques*, Ph.D., Archeologia dept. Pisa Univ., Italy.
- [20] Lucas, A. (2003). *Ancient Egyptian materials and industries*, 3rd ed., Edward Arnold & Co, London.
- [21] Mora, P., Mora, L. & Philippot, P. (1984). *Conservation of wall painting*, ICCROM, Italy.
- [22] Eastaugh, N., Walsh, V., Chaplin, T., et al. (2004). *The pigment compendium: A dictionary of historical pigments*. Butterworth-Heinmann, Oxford.
- [23] Akarish, A., Shoeib, A. & Suita, H., (2010). Characterization of some inorganic pigments and plasters used in old kingdom, Saqqara area, Egypt, *J. Institute for Conservation and Restoration of Cultural Properties*, Vol. 2, Kansai Univ., Japan, pp. 17-27.
- [24] Mancini, A. & Hefni, Y. (2020). Analytical study of wall paintings at monastery of ST. Macarius of Alexandria, Egypt, *J. of Engineering and Applied Science*, Cairo Univ., Vol. 67 (7), pp. 1535-1554.
- [25] Abdelaal, Sh. (2014). Characterization and examination of pigments, grounds and media from ancient Egyptian cartonnage, *EJARS*, Vol. 4 (1), pp. 35-46.
- [26] Abdelaal, Sh. Mahmoud, N. & Detalle, V., (2014). A technical examination and the identification of the wood,

- pigments, grounds and binder of an ancient Egyptian sarcophagus, *IJCS*, Vol. 5 (2), pp. 177-188.
- [27] Lucas, A. & Harris, J. (2001). *Ancient Egyptian Materials and Industries*, 4th ed., Dover Pub. INC, NY.
- [28] Siddall, R. (2018). Mineral pigments in archaeology: Their analysis and the range of available materials, *J. of Minerals*, Vol. 8 (5), doi: 10.3390/min8050201
- [29] Ali, M., Abdel-Ghani, M & Abou Seif, N. (2022). An analytical study of a late period multi-piece cartonnage from the Egyptian museum in Cairo, *EJARS*, Vol. 12 (1), pp. 29-40.
- [30] Ali, M., Moussa, A & El-Sayed, S. (2022). Analytical physicochemical survey of the recently excavated murals at the tomb of Iwrakhy/Hatia at Saqqara, Egypt, *Scientific Culture*, Vol. 8 (1), pp. 63-79.
- [31] El-Gohary, M. (2011). Analytical investigations of disintegrated granite surface from the Un-finished obelisk in Aswan, *Int. J. of Archaeo-Science*, Vol. 35, pp. 29-39.
- [32] Coccato, A., Jehlicka, J., Moens, L., et al. (2015). Raman spectroscopy for the investigation of carbon-based black pigments, *J. of Raman Spectrosc.*, Vol. 46, pp. 1003-1015.
- [33] Winter, J. (1983). The characterization of pigments based on carbon, *Studies in Conservation*, Vol. 29 (1), pp. 59-69.
- [34] Hatton, G., Shortland, A., Tite, M. (2008). The production technology of Egyptian blue and green frits from second millennium BC Egypt and Mesopotamia, *J. of Archaeological Science*, Vol. 35 (6), pp. 1591-1604.
- [35] Barnett, J., Miller, S. & Pearce, E., (2006). Colour and art: A brief history of pigments, *Optics & Laser Technology*, Vol. 38 (4-6), 2006, pp. 445-453.
- [36] Marye, H., Nikolaos, K., Ali, M., et al. (2011). Characterization of ancient Egyptian wall paintings, The excavations of Cairo University at Saqqara, *IJCS*, Vol. 2 (3), pp. 145-154.
- [37] Al-Emam, E, El-Gohary, M. & Abd El Hady, M. (2015). The paint layers of mural paintings at Abydos temples-Egypt: A closer look at the materials used, *MAA*, Vol. 15 (3), pp. 113-121.
- [38] Afifi, H., Etman, M., Abdrabbo, H., et al. (2020). Typological study and non-destructive analytical approaches used for dating a polychrome gilded wooden statuette at the grand Egyptian museum, *Scientific Culture*, Vol. 6 (3), pp. 69-83.
- [39] Badr, N. & Mahran, A. (2012). Analytical investigation of cartonnage fragment from late period, *EJARS*, Vol. 2 (2), pp. 69-78.
- [40] Abdel-Ghani, M. (2009). *A multi-instrument investigation of pigments, binders and varnishes from Egyptian paintings (AD 1300-1900): Molecular and elemental analysis using Raman, GC-MS and SEM-EDX techniques*, Ph.D., Univ. of Bradford, UK
- [41] Sakr, A., Ghaly, M., Abdulla, M., et al. (2020). A new light on the grounds, pigments and bindings used in ancient Egyptian cartonnages from Tell Al Sawa, Eastern Delta, Egypt, *J. of Optics*, Vol.49 (2), pp. 230-247.
- [42] Dziejczak, T., Bartz, W. & Gąsior, M. (2015). Mineralogical characteristic of mortars from the temple of Hatshepsut at El Deir el Bahari: Preliminary report, *Polish Archaeology in Mediterranean*, Vol. 24 (2), pp. 39-111.
- [43] Shoeib, A., Aboelala, A., Mancy, A. (2017). Technical characterization of the mural paintings in the burial chamber of Mereruka tomb, Saqqara, Egypt, *J. of Center for the Global Study of Cultural Heritage and Culture*, Vol. 5, pp. 1-16.
- [44] Laboury, D. (2010). Les artistes des tombes privées. De la nécropole Thébaine sous la XVIII^e dynastie: Bilan et perspectives, *EAO*, Vol. 59, pp. 33-46.

- [45] Singh, M. & Arbad, B. (2014). Ancient Indian painting recipes and mural art technique at Ajanta, *IJCS*, Vol. 5 (1), pp. 35-50.
- [46] Dawson, J. (2001). Conservation of the 'tombs of the nobles': Aspects of the past, issues for the present, in: Davies, W. (ed.) *Colour and Painting in Ancient Egypt*, The British Museum Press, London:, pp. 210-217.
- [47] Orabi, E. & Sallam, A. (2022). Damage assessment and nano treatment of the Sharia Judge tomb at the Fatimid cemetery, Aswan-Egypt, *EJARS*, Vol. 12 (2), pp. 217-225.
- [48] Abdel Aal, Sh. (2019). Investigation and identification of mural paintings materials and techniques in Ain El-Lepekha, Egypt - Part one, *EJARS*, Vol. 9 (2), pp. 171-181.
- [49] Behlmer, H (2007). Christian use of pharaonic sacred space in western Thebes: The case of TT 85 and 87, in: Dorman, P. & Bryan, B. (eds.) *Sacred space and sacred function in ancient Thebes*, Oriental Institute of the Chicago Univ., Chicago: pp. 163-175.
- [50] EL-Fakharany, M. (1998). Drainage Basins and flash floods, management in the area southeast Qena Eastern desert, *Egyptian, J. of Geol.*, Vol. 42 (2), pp. 737-750.
- [51] Wüst, R. & McLane, J., (2000). Rock deterioration in the royal tomb of Seti I, Valley of the Kings, Luxor, Egypt, *Engineering Geology*, Vol. 58, pp. 163-190.
- [52] Wüst, R. & Schlüchter, C. (2000). The origin of soluble salts in rocks of the Thebes Mountains, Egypt: The damage potential to ancient Egyptian wall art, *J. of Archaeological Science*, Vol. 27, pp. 1161-1172.
- [53] Akarish, A. & Shoeib, A. (2011). The role of rock composition in the deterioration of wall paintings, Saqqara area, Egypt: Information from petrography and mineralogy, *Australian J. of Basic and Applied Sciences*, Vol. 5 (5), pp.1144-1153.
- [54] Moussa, A., Kantiranis, N., Voudouris, K. et al. (2009). The impact of soluble salts on the deterioration of pharaonic and Coptic wall paintings at Al Qurna, Egypt: Mineralogy and chemistry, *Archaeometry*, Vol. 51, pp. 292- 308.
- [55] Moussa, A. & Roshdy, M. (2021). Monitoring Coptic masonry affected by clay minerals and microorganisms at the church of Virgin Mary, Wadi El-Natron (Egypt), *Heritage*, Vol. 4, pp. 4056-4067.
- [56] Abdelfatah, M., Kamal, M. & Fahmy, H. (2017). The role of geotechnical properties of rocks in failure of stability of the funeral subsurface structures in Saqqara plateau, Egypt: Part 1, *J. of Center for the Global Study of Cultural Heritage and Culture*, Vol. 5, pp. 103-116.
- [57] Abdelaal. Sh., Yamani. R., Abdel fatah. M., et al. (2019). Salt weathering of Imni tomb: Proplem identification and characterization, *IJCS*, Vol. 10 (4), pp. 661-680.
- [58] Baderi, N. & Abu El-Hassan. R., (2021). Technical examination and state of conservation of wall painting at the Theban tomb TT15 at Dra' Abu El-Naga necropolis, western Thebes, Luxor, Egypt, *IJCS*, Vol. 12 (4), pp. 1391-1406.
- [59] Beskhyroun, S., Mahgoub, G., El-Rifai, I., et al. (2019). Study of the painted dome of the church of Archangel Gabriel, Cairo, *EJARS*, Vol. 9 (2), pp. 129-140.
- [60] Afifi, H., Hassan, R. & Menofy, S. (2021). An experimental study for consolidation of archaeological cartonnage using Klucel G and Chitosan, with nanocalcium hydroxide, *Scientific Culture*, Vol. 7 (2), pp. 49-68.
- [61] Lardet, G. (2014). Comparaison du Plexisol® P550 et du medium de consolidation® 4176, <https://journals.openedition.org/ceroart/3986> (10-5-2023)
- [62] Shoeib, A. Shakal, A. & Abd El-Latif, M. (2016). Comparison between

- nanolime and Plexisol P550 as two consolidants for the preservation of humidity saturated monumental limestone, *J. of Center for the Global Study of Cultural Heritage and Culture*, Vol. 4, pp. 255-268.
- [63] Brus, J. & Kotlík, P. (1996). Consolidation of stone by mixtures of alkoxy silane and acrylic polymer, *Studies in Conservation*, Vol. 41, (2), pp. 109-119.
- [64] Saleh, S, Helmi, F. Kamal, M., et al. (1992). Study and consolidation of sandstone: Temple of karnak, Luxor, Egypt, *Studies in Conservation*, Vol. 37 (2) pp. 93-104.
- [65] El-Gohary, M. (2015). Methodological evaluation of some consolidants interference with ancient Egyptian sandstone “Edfu Mammisi as a case study”, *Progress in Organic Coatings*, Vol. 80, pp. 87-97.
- [66] Allen, N., Edge, M. & Horie, C. (1992). *Polymers in conservation*, The Royal Society of Chemistry, Cambridge.
- [67] Sallam, M., Marouf, M., El Hadidi, N., et al. (2022). Evaluation of using Klucel G on the physical properties of sycamore wood, *Int. J. of Multidisciplinary Studies in Architecture and Cultural Heritage*, Vol. 5 (1), pp. 135-139.
- [68] Hassan, L. (2022). Reintegration technique (Missing parts): In conservation-restoration of antiquities», *Int. J. of Archaeology*, Vol. 10 (2), pp. 38-45.
- [69] Orabi, E. & Abu Elyameen, A. (2020). analytical study and treatments of the decayed mural paintings at Athribis in Sheikh Hamad temple, Sohag governorate, Egypt, *Shedet*, Vol. 7, pp. 238-249.